A Simple Model for Stratified Shelf Flow Fields with Bottom Friction

J. S. ALLEN

College of Oceanography, Oregon State University, Corvallis, OR 97331.

(Manuscript received 25 July 1983, in final form 1 May 1984)

ABSTRACT

The effect of bottom friction on the subinertial frequency motion of stratified shelf flow fields is studied in a two-layer f-plane model with idealized shelf and slope bottom topography. Coastal-trapped free waves and motion forced by the alongshore component of the wind stress at the coast are considered. Vertical turbulent-diffusion effects are assumed to be present in thin surface and bottom-boundary layers, but not at the density interface. Simplifications are achieved by assuming that typical alongshore scales are larger than the offshore scales given by the internal Rossby radius of deformation δ_R and the shelf-slope width, that the upper-layer depth is small compared with the lower-layer depth, and that the topography of the continental margin may be represented by a linear bottom slope of small magnitude. Some results are not dependent on the presence of variable bottom topography; these are obtained first with a flat-bottom ocean adjacent to a vertical coast. A characteristic feature of free and forced motion with alongshore gradients is a decrease of lower-layer velocity and a resultant concentration of flow in the upper layer as the frequency approaches zero. For internal Kelvin waves of frequency ω, this change in velocity structure occurs for $\omega/\alpha \ll 1$, where α^{-1} is barotropic spin-down time, and is accompanied by a decrease in frictional decay as $\omega/\alpha \to 0$. As a result, coastal internal Kelvin waves may be able to participate with relatively small damping by bottom friction in low-frequency phenomena such as El Niño. For motion forced at frequency σ and alongshore wavenumber l, this change in structure occurs for $\sigma/\alpha \ll 1$ and $\sigma(l\delta_R)^{-1} \ll 1$. Concurrently, the magnitude of the barotropic, forced-shelf-wave component of the flow goes to zero as $\sigma \to 0$. Thus, the "arrested topographic wave" is absent and plays no role in the steady solutions. Qualitatively similar behavior is found on the Oregon shelf in the summer where monthly mean alongshore currents at midshelf have substantial vertical shear, but corresponding fluctuations on the several-day time scale are nearly depth-independent. Generalized first-order wave equations are derived to describe the alongshore (y) and time (t) dependence of the lowest-order baroclinic and barotropic components. The response to a wind stress with Heaviside-unit-function behavior in both y and t clearly illustrates how the effects of stratification liberate the "arrested topographic wave" and how a steady state is achieved where the currents are confined to the upper layer and to a region near the coast with offshore scale of $O(\delta_R)$.

1. Introduction

A fairly complete set of models and illustrative solutions exists for linear, barotropic shelf flow fields under a variety of different conditions. These include the effects of realistic cross-shelf topography, alongshore variations in wind stress, alongshore variations in bottom topography, and bottom friction (see, e.g., Allen, 1980). The set of existing models of stratified shelf flow fields, however, is far less complete. For example, the effect of bottom friction on stratified shelf flow is not well understood. Because both stratification and bottom friction undoubtedly play important roles on many shelves, it is desirable to expand the set of simple models to include the combined action of these two processes. This is especially so because the fundamental characteristics of the flow in that case are likely to differ considerably from those of barotropic models.

In this paper, we formulate a simple two-layer model for the effect of bottom friction on stratified shelf flow fields. The geometry is highly idealized; a vertical coast is utilized and the continental margin is represented by a linear bottom slope of small amplitude. Free and wind-stress-forced coastal-trapped motions are investigated. Several features of interest are not dependent on bottom slope; these are investigated first with a flat-bottom ocean, adjacent to a vertical coast. Further simplifications in the analysis are achieved by the assumptions that the upper-layer depth is small compared with the lower-layer depth and that alongshore spatial scales are larger than onshore–offshore scales.

Although the model is highly idealized, it retains the basic effects of stratification, a coastal boundary and sloping shelf topography, and it allows one to obtain simple analytical solutions that are substantially different from those found without friction and those in the purely barotropic case. The results obtained, in fact, provide explanations for the basic qualitative behavior of currents on the Oregon shelf for which previous dynamical rationalizations have been lacking.

Those observations are discussed in Section 5, along with the limitations of the model and the relationship of this study to previous work.

2. Formulation

We consider a two-layer model on an f-plane. Cartesian coordinates (x', y', z') are utilized with z' positive vertically upward. Stratification is modeled by two layers of homogeneous fluids of different density, with the heavier fluid on the bottom. The top surface is bounded by a horizontal rigid lid. The upper-layer fluid has density ρ_1 and a constant undisturbed depth H_1'. The lower layer has density ρ_2 and a variable undisturbed depth $H_2'(x')$. The total depth is $H' = H_1' + H_2'$. The difference in density $\Delta\rho = \rho_2 - \rho_1$ is assumed to be small: $\Delta\rho \ll \rho_2$.

The fluid is bounded by a straight coastline at $x' = 0$. In the initial examples in Section 3, the coastal boundary is a vertical wall and the interior is of constant depth $H' = H_0' = H_1' + H_{20}'$. In later cases in Section 4, idealized, y-independent continental shelf and slope topography of width L lies along the coast at $x' = 0$, so that $H' = H'(x')$ for $0 \leq x' \leq L$ and $H' = H_0'$ for $x' \geq L$. We concentrate on examining the free and wind-stress-forced coastal-trapped motions.

The flow is assumed to be linear and hydrostatic. Vertical turbulent diffusion is assumed to be active in surface and bottom boundary layers, but not at the density interface. The latter assumption is made in order to model the frictional effects that are most likely to be dominant.

Dimensionless variables are formed in the following manner:

$$(x, y) = (x', y')/L, \quad t = t'f,$$

$$(u_i, v_i) = (u_i', v_i')/U,$$

$$p_1 = [p_1' + \rho_1 g(z' - H_0')]/(\rho_1 UfL),$$

$$p_2 = [p_2' + \rho_2 g(z' - H_{20}') - \rho_1 g H_1']/(\rho_2 UfL),$$

$$h = h' g\Delta\rho/(\rho_2 UfL),$$

$$(H_1, H_2, H) = (H_1', H_2', H')/H_0',$$

$$\tau^{x,y} = \tau'^{x,y}/\tau_C,$$

$$\tau_B^{x,y} = \tau_B'^{x,y}/(\rho_2 UfH_0'),$$

where subscripts $i = 1, 2$, denote variables in the upper and lower layers, respectively. The variables (u', v') are the depth-averaged velocity components in the (x', y') directions, p' is the pressure, h' the height of the density interface above H_{20}', $\tau'^{x,y}$ and $\tau_B'^{x,y}$ the surface wind-stress and bottom-stress components, respectively, in the (x', y') directions, t' is time, f the Coriolis parameter, g the gravitational acceleration, L is a characteristic offshore scale, U a characteristic velocity, and $\tau_C = \rho_2 UfH_1'$, a characteristic wind stress.

The linear depth-averaged continuity and momentum equations in dimensionless variables (e.g., Allen, 1975) are

$$(H_1u_1)_x + (H_1v_1)_y = S^{-1}h_t, \tag{2.1a}$$

$$u_{1t} - v_1 = -p_{1x} + \tau^x, \tag{2.1b}$$

$$v_{1t} + u_1 = -p_{1y} + \tau^y, \tag{2.1c}$$

$$(H_2u_2)_x + (H_2v_2)_y = -S^{-1}h_t, \tag{2.1d}$$

$$u_{2t} - v_2 = -p_{2x} - \tau_B^x H_2^{-1}, \tag{2.1e}$$

$$v_{2t} + u_2 = -p_{2y} - \tau_B^y H_2^{-1}, \tag{2.1f}$$

where subscripts (x, y, t) denote partial differentiation,

$$h = p_2 - p_1, \tag{2.1g}$$

$$S = (NH_0'/fL)^2, \quad N^2 = g\Delta\rho/(\rho_2 H_0'). \tag{2.2a,b}$$

We consider motions on a time scale δ_t which is large compared with an inertial period, i.e., where

$$\delta_t \gg 1. \tag{2.3}$$

The sum of (2.1a) and (2.1d) allows a streamfunction ψ to be defined such that

$$\psi_y = u_1 + a^{-1}u_2, \quad -\psi_x = v_1 + a^{-1}v_2, \tag{2.4a,b}$$

where

$$a = H_1/H_2. \tag{2.5}$$

In terms of ψ and h, the velocity components are [with assumption (2.3)]

$$u_1 = (H_1/H)(\psi_y + a^{-1}F), \tag{2.6a}$$

$$v_1 = (H_1/H)(-\psi_x - a^{-1}G), \tag{2.6b}$$

$$u_2 = (H_1/H)(\psi_y - F), \tag{2.6c}$$

$$v_2 = (H_1/H)(-\psi_x + G), \tag{2.6d}$$

where

$$F = h_y + h_{xt} + H_2^{-1}\tau_B^y + \tau^y, \tag{2.6e}$$

$$G = h_x + [-h_{yt} + H_2^{-1}\tau_B^x + \tau^x]. \tag{2.6f}$$

The brackets in (2.6f) enclose terms that in Section 4 are small on the continental shelf and slope under assumptions (2.3) and (2.11) (see Appendix A).

Equations (2.1) may be combined into two equations for the variables ψ and h. With $H = H(x)$ and (2.3), these are

$$(\psi_{xx} + \psi_{yy} - \delta_B^{-1}\psi_x)_t + \delta_B^{-1}(\psi_y - h_y - \tau^y) - (H/H_1)(\tau_B^y/H)_x + H_1^{-1}\tau_{By}^x = \tau_y^x - \tau_x^y, \tag{2.7a}$$

$$(h_{xx} + h_{yy} + a\delta_B^{-1}h_x - \delta_R^{-2}h)_t - a\delta_B^{-1}(\psi_y - h_y - \tau^y) + a(H/H_1)(\tau_B^y/H)_x - aH_1^{-1}\tau_{By}^x = \tau_y^x - \tau_x^y, \tag{2.7b}$$

where $\delta_B^{-1} = H_x/H$, $\delta_R^2 = S\bar{H}$, $\bar{H} = H_1H_2/H$ and δ_R is the internal Rossby radius of deformation.

The bottom-stress components $\tau_B^{x,y}$ are assumed to be linearly related to the inviscid horizontal velocity components above the bottom boundary layer (u_{2A},

v_{2A}) in a manner consistent with a linear, constant-eddy-coefficient Ekman layer with thickness δ_E' small compared to the lower-layer depth H_2':

$$\tau_B{}^x = \alpha(u_{2A} - v_{2A}), \quad \tau_B{}^y = \alpha(u_{2A} + v_{2A}), \quad (2.8a,b)$$

$$u_{2A} = u_2 + (\tau_B{}^y/H_2), \quad v_{2A} = v_2 - (\tau_B{}^x/H_2), \quad (2.8c,d)$$

where $\alpha = \frac{1}{2}\delta_E'/H_0'$, $\delta_E' = (2A_v/f)^{1/2}$, A_v is the vertical eddy viscosity, and

$$\alpha \ll 1. \quad (2.9)$$

Utilizing (2.9) together with (2.8) and (2.6), we find $\tau_B{}^{x,y} = O(\alpha)(u_2, v_2)$. Thus, for use in (2.8a, b) we obtain the approximations

$$u_{2A} = (H_1/H)(\psi_y - h_y - h_{xt} - \tau^y), \quad (2.10a)$$

$$v_{2A} = (H_1/H)(-\psi_x + h_x - [h_{yt} - \tau^x]), \quad (2.10b)$$

with error $O(\alpha)$.

We will assume that a typical alongshore scale δ_y is large compared with the O(1) offshore scales given by the internal Rossby radius of deformation δ_R and the shelf–slope width, i.e., that

$$l_0 \ll 1, \quad (2.11)$$

where $l_0 = 2\pi/\delta_y$ is a typical alongshore wavenumber.

We will also assume that the upper-layer depth H_1 is small compared to the lower-layer depth H_2, i.e., that

$$a = H_1/H_2 \ll 1. \quad (2.12)$$

In addition, the continental shelf and slope topography will be represented by a "weak slope" model with a linear bottom slope of small magnitude (see Fig. 1). In this case

$$H = 1 + \delta_B{}^{-1}(x - 1), \quad H_x = \delta_B{}^{-1} \ll 1, \quad (2.13a,b)$$

δ_B is a constant, and in (2.7) H_2 and H are regarded as constants (where not differentiated). The assumptions (2.12) and (2.13) are made because they appear to retain, respectively, the most essential features of stratification and sloping bottom topography while at the same time they allow very simple analytical solutions to be obtained. In particular, assumption (2.12) permits the effects in a two-layer model of variable bottom topography to be readily taken into account by a perturbation procedure (Allen and Romea, 1980). With (2.12), the baroclinic component of the flow does not feel the effect of the bottom topography at lowest order in a. The weak-slope approximation (2.13) is made here primarily to allow the *barotropic* component of the solution to be obtained analytically for all ranges of the ratio of frequency to bottom-friction coefficient ω/α. In addition, it has the advantage of approximating all otherwise x-dependent coefficients as constants, which permits exact analytical solutions to be obtained. Since the basic effects of stratification and bottom slope are retained, it is hoped that qualitative results from the model will apply even when the assumptions are not strictly satisfied.

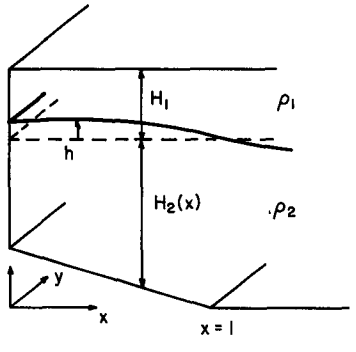

FIG. 1. Geometry of the "weak slope" model.

When the weak-slope model is utilized, we will restrict our analysis to the midlatitude case where δ_R is smaller than the width of the shelf and slope, i.e., where

$$\delta_R \ll 1. \quad (2.14)$$

In addition, for simplicity in the forced problems and to focus on the motion forced by the Ekman divergence at the coast, we will assume

$$\tau^y \neq 0, \quad \tau^x = 0, \quad (2.15a,b)$$

and in most cases

$$\tau_x{}^y = 0. \quad (2.15c)$$

3. Flat bottom

Some of the basic effects of bottom friction in a stratified coastal region are illustrated in the case of a flat-bottom ocean bounded by a vertical coast at $x = 0$. With $H = 1$, assumptions (2.3), (2.9), (2.11), $\tau^x = 0$ and $\tau^y = \tau$, Eqs. (2.7) become

$$\nabla^2\psi_t + \alpha\nabla^2(\psi - h) = \alpha\tau_y - \tau_x, \quad (3.1a)$$

$$(\nabla^2 h - \delta_R{}^{-2}h)_t - a\alpha\nabla^2(\psi - h) = -a\alpha\tau_y - \tau_x, \quad (3.1b)$$

where $\nabla^2\psi = \psi_{xx} + \psi_{yy}$. Note that bottom friction acts on both the barotropic ψ- and baroclinic h-components of the flow through the term $\nabla^2(\psi - h)$ representing lower-layer vorticity. At the coast, the boundary conditions on ψ and h follow from the requirement that $u_1 = u_2 = 0$ and are

$$\psi_y = 0, \quad (3.2a)$$

$$h_y + h_{xt} - \alpha a(\psi_x - h_x) = -\tau \quad \text{at} \quad x = 0. \quad (3.2b)$$

In addition, we require

$$\psi_x, \psi_y, h_x, h_y \quad \text{bounded as} \quad x \to \infty. \quad (3.3)$$

a. Free waves

We first consider $\tau = 0$ and look for free coastal-trapped wave solutions of (3.1), (3.2) and (3.3) in the form

$$(\psi, h) = [\phi(x), g(x)] \exp(i\omega t + ily), \quad (3.4)$$

with $l \geqslant 0$. We obtain

$$\phi = C_1\hat{\alpha}(e^{-rx} - e^{-lx}), \quad (3.5a)$$

$$g = C_1 e^{-rx}, \quad (3.5b)$$

$$\omega = r^{-1}l(1 + ia\alpha\hat{\alpha})(1 + a\hat{\alpha})^{-1}, \quad (3.6a)$$

$$r = \delta_R{}^{-1}(1 + a\hat{\alpha})^{-1/2}, \quad \hat{\alpha} = \alpha(i\omega + \alpha)^{-1}, \quad (3.6b,c)$$

where small terms $O(l^2\delta_R{}^2)$ have been neglected.

For $a \ll 1$, i.e., with assumption (2.12), the expressions in (3.6) simplify and may be readily solved for a frictionally modified internal Kelvin wave. Neglecting terms $O(a^2)$, we obtain

$$\omega = \omega_R + i\omega_I, \quad (3.7a)$$

$$\omega_R = \omega_0\left(1 - \tfrac{1}{2}a\alpha^2 d\right), \quad (3.7b)$$

$$\omega_I = \omega_0 a\alpha d\left(\tfrac{1}{2}\omega_0 + \alpha^2\right), \quad (3.7c)$$

where

$$\omega_0 = \delta_R l \ll 1, \quad d = (\omega_0{}^2 + \alpha^2)^{-1},$$

and

$$r = r_R + ir_I, \quad (3.8a)$$

$$r_R = \delta_R{}^{-1}\left(1 - \tfrac{1}{2}a\alpha^2 d\right), \quad (3.8b)$$

$$r_I = \tfrac{1}{2}\delta_R{}^{-1}a\alpha\omega_0 d. \quad (3.8c)$$

Note that an attractive feature of the $a \ll 1$ approximation is that the expansions (3.7) and (3.8) remain uniformly valid for all values of ω_0/α.

For $(\omega_0/\alpha)^2 \gg 1$, (3.7b, c) give

$$\omega_R \sim \omega_0\left[1 - \tfrac{1}{2}a(\alpha/\omega_0)^2\right], \quad (3.9a)$$

$$\omega_I \sim \tfrac{1}{2}a\alpha. \quad (3.9b)$$

The $O(a)$ modification to ω_R corresponds to a decrease in wave speed, whereas ω_I results in a constant exponential decay in time with timescale $T_F = \omega_I{}^{-1} = 2(a\alpha)^{-1}$. For comparison, the barotropic spin-down time is $T_{BF} = \alpha^{-1}$ so that with $a \ll 1$, $T_F \gg T_{BF}$.

For $(\omega_0/\alpha)^2 \ll 1$, (3.7b, c) imply

$$\omega_R \sim \omega_0\left(1 - \tfrac{1}{2}a\right), \quad (3.10a)$$

$$\omega_I \sim \omega_0 a\left[\tfrac{1}{2}(\omega_0/\alpha) + \alpha\right]. \quad (3.10b)$$

The wave speed is again reduced and the reduction is greater than in the high-frequency limit (3.9a). Also, in contrast to (3.9b), ω_I varies with ω_0 such that as $\omega_0 \to 0$ frictional effects vanish, i.e., $\omega_I \to 0$. In particular, for waves of period $T = 2\pi/\omega_0$, the decay timescale $T_F \approx T(2\pi a\alpha)^{-1}$ as $\omega_0 \to 0$. Moreover, for $\frac{1}{2}\omega_0 > \alpha^2$, ω_I decreases as the friction coefficient α increases. The reason for this behavior may be seen by examining the velocity components. Using the notation

$$(u_i, v_i) = (\tilde{u}_i, \tilde{v}_i) \exp(i\omega t + ily),$$

we obtain for $(\omega_0/\alpha)^2 \ll 1$,

$$\tilde{u}_2 \sim C_1 H_1 il\hat{\alpha}(e^{-rx} - e^{-lx}), \quad (3.11a)$$

$$\tilde{v}_2 \sim C_1 H_1 l[(-i\hat{\alpha}\alpha^{-1} + \omega_0)e^{-rx} - \hat{\alpha}e^{-lx}], \quad (3.11b)$$

$$\tilde{v}_1 \sim C_1 H_2 \delta_R{}^{-1} e^{-rx}[1 + O(a)]. \quad (3.11c)$$

Thus, as $\omega_0 = \delta_R l \to 0$, the velocity components in the lower layer $\tilde{u}_2, \tilde{v}_2 \to 0$, concentrating the velocity fluctuations in the upper layer and reducing the effect of bottom friction. This is caused by the requirement from (3.1) that as $\omega \to 0$ the lower-layer vorticity must vanish.

Examination of (3.8) shows that relative to the case of no bottom friction the offshore decay scale $r_R{}^{-1}$ is increased. Also, since $r_I/\omega_0 > 0$ an offshore phase propagation is induced with nearshore fluctuations leading those offshore. Results similar to these have been found for the effect of bottom friction on barotropic Kelvin waves (Mofjeld, 1980).

Vertical phase relations dependent on ω_0/α are also generated. Looking at those parts $\bar{v}_i$ of v_i that vary as e^{-rx} we obtain

$$\bar{v}_2/a\bar{v}_1 = \omega_0 d^{1/2} \exp\{i[\pi + \tan^{-1}(\alpha/\omega_0)]\}. \quad (3.12a)$$

For $(\omega_0/\alpha)^2 \gg 1$,

$$\bar{v}_2/a\bar{v}_1 \sim \exp(i\pi). \quad (3.12b)$$

In this limit, $\bar{v}_2$ and $\bar{v}_1$ are π out of phase, as with zero friction. For $(\omega_0/\alpha)^2 \ll 1$,

$$\bar{v}_2/a\bar{v}_1 \sim (\omega_0/\alpha)\exp\left(-i\tfrac{1}{2}\pi\right), \quad (3.12c)$$

and $\bar{v}_2$ lags $\bar{v}_1$ by $\frac{1}{2}\pi$.

b. Forced response

Assuming a wind stress

$$\tau^y = \tau = \tau_0 \exp(i\sigma t + ily + i\kappa x), \quad (3.13)$$

($l \geqslant 0$), and looking for solutions of (3.1) and (3.2) of the form

$$(\psi, h) = (\phi, g) \exp(i\sigma t + ily), \quad (3.14a)$$

we obtain

$$\phi = C_1\hat{\alpha}(e^{-rx} - e^{-lx}) + K_2(e^{i\kappa x} - e^{-lx}), \quad (3.14b)$$

$$g = C_1 e^{-rx} + K_1 e^{i\kappa x}, \quad (3.14c)$$

where

$$\hat{\alpha} = \alpha(i\sigma + \alpha)^{-1}, \quad (3.14d)$$

$$K_1 = \tau_0\delta_R{}^2[\kappa\sigma^{-1}(1 - a\hat{\alpha}) + ial\hat{\alpha}], \quad (3.14e)$$

$$K_2 = K_3 + \hat{\alpha}K_1, \quad (3.14f)$$

$$K_3 = i\tau_0\alpha^{-1}\hat{\alpha}(\kappa - al)(\kappa^2 + l^2)^{-1}, \quad (3.14g)$$

$$irC_1(-\sigma + \omega) = -\tau_0 + (\sigma\kappa - il)K_1 + a\alpha[(i\kappa + l)K_2 - i\kappa K_1]; \quad (3.14h)$$

r and ω remain defined by (3.6a, b), but (3.14d) replaces (3.6c).

The nature of the forced response may be seen most easily by examining different limiting cases. For simplicity, we are primarily interested in the case $\kappa = 0$ so that $\tau_x^y = 0$. It is useful, however, to keep $\kappa \neq 0$ in the initial formulation to allow the easy derivation of proper limiting solutions. Thus, the correct two-dimensional ($l = 0$) solution with $\kappa = 0$ may be obtained by taking the limits $l \to 0$, $\kappa \to 0$, in that order. For convenience in the following discussion, we define

$$(u_i, v_i) = (\tilde{u}_i, \tilde{v}_i)\exp(i\sigma t + ily).$$

1) TWO-DIMENSIONAL FLOW, $l = 0$

Taking the limits $l \to 0$, $\kappa \to 0$ in order, we find

$$\phi_x \approx -(\tau_0/i\sigma)\hat{\alpha}e^{-rx}[1 + O(a)] - \tau_0\hat{\alpha}/\alpha, \quad (3.15a)$$

$$g_x \approx -(\tau_0/i\sigma)e^{-rx}[1 + O(a)], \quad (3.15b)$$

and to O(1),

$$\tilde{u}_1 \approx H_2\tau_0(1 - e^{-rx}), \quad (3.16a)$$

$$\tilde{v}_1 \approx H_2(\tau_0/i\sigma)e^{-rx}, \quad (3.16b)$$

$$\tilde{u}_2 \approx -a\tilde{u}_1, \quad (3.16c)$$

$$\tilde{v}_2 \approx H_1[\tau_0/(i\sigma + \alpha)](1 - e^{-rx}). \quad (3.16d)$$

As $\sigma/\alpha \to 0$, u_1, u_2 and v_2 reach a steady state, but v_1 is unbounded. This reflects the fact that in two-dimensional flow with bottom friction a steady forced solution for h and v_1 does not exist within a frictionally modified Rossby radius of the coast. A similar result is obtained in continuously stratified two-dimensional models when bottom friction is the only dissipative mechanism (e.g., Allen, 1973).

Far from the coast ($x \gg r^{-1}$) we find, without approximation in a, that $\phi_x \sim -\tau_0\hat{\alpha}/\alpha$, $g_x \sim 0$. Thus, $\tilde{u}_1$, $\tilde{u}_2$ may be readily evaluated there to O(a) by including the bottom-stress terms. We obtain $\tau_B^y \sim H_1\tau_0\hat{\alpha}$ and

$$\tilde{u}_2 \sim -H_1\tau_0(1 + a\hat{\alpha}), \quad \tilde{u}_1 \sim -a\tilde{u}_2.$$

In the limit $\sigma/\alpha \to 0$, this gives

$$\tilde{u}_2 \sim -a\tau_0 = -\tau_B^y/H_2, \quad \tilde{u}_1 \sim \tau_0,$$

which corresponds to offshore (onshore) transport in the surface Ekman layer balanced by an onshore (offshore) transport in a bottom Ekman layer. Within r^{-1} of the coast, upwelling (downwelling) occurs, involving a necessarily time-dependent motion of the density interface and of the upper-layer alongshore velocity.

Note that for fixed σ, an increase in the friction coefficient decreases $|\tilde{v}_2|$, but does not affect $|\tilde{v}_1|$ to O(1) so that the vertical shear is increased.

In the purely two-dimensional case with $\tau^y = \tau_0 \times \exp(i\sigma t)$, as above, an approximate solution for $a \ll 1$ may be readily obtained for fairly general shelf and slope topography $H(x)$. That solution is given in Appendix B.

In the following examples, we consider the limit $\kappa \to 0$ with $l \neq 0$, in which case

$$K_1 = a\delta_R{}^2l^2K_3, \quad (3.17a)$$

$$K_2 = K_3 + \hat{\alpha}K_1, \quad K_3 = -i\tau_0\hat{\alpha}/l. \quad (3.17b,c)$$

2) FRICTIONLESS, $\alpha = 0$, $l \neq 0$

For $\alpha = 0$, $l \neq 0$, we obtain

$$K_1 = K_2 = K_3 = 0, \quad C_1 = (i\tau_0/l)(1 - \sigma/\omega_0)^{-1},$$

so that

$$\tilde{u}_1 = H_2\tau_0[1 - (1 - \sigma/\omega_0)^{-1}e^{-rx}], \quad (3.18a)$$

$$\tilde{v}_1 = H_2(i\tau_0/l)(1 - \sigma/\omega_0)^{-1}re^{-rx}, \quad (3.18b)$$

$$\tilde{u}_2 = -a\tilde{u}_1, \quad \tilde{v}_2 = -a\tilde{v}_1. \quad (3.18c,d)$$

Far from the coast,

$$x \gg r^{-1}, \quad \tilde{u}_1 \sim H_2\tau_0, \quad u_2 \sim -H_1\tau_0,$$

so that the y-dependent offshore (onshore) surface Ekman-layer transport is balanced locally by an onshore (offshore) barotropic flow. The circulation is completed by baroclinic motion within a Rossby radius of the coast. Note that for the forcing frequency $\sigma \to 0$,

$$\tilde{u}_1 = H_2\tau_0[1 - e^{-rx}], \quad (3.19a)$$

$$\tilde{v}_1 = H_2(i\tau_0/l)re^{-rx}, \quad (3.19b)$$

$$\tilde{u}_2 = -a\tilde{u}_1, \quad \tilde{v}_2 = -a\tilde{v}_1, \quad (3.19c,d)$$

so that for $l \neq 0$ a steady, frictionless solution exists. In this case, a barotropic onshore (offshore) flow still balances the Ekman transport far from the coast, but because alongshore pressure gradients are set up in response to alongshore variations in τ the circulation in each layer may be closed independently by a steady geostrophic flow, with no time-dependent motion of the density interface required.

3) FRICTIONAL STEADY STATE $\alpha \neq 0$, $l \neq 0$, $\sigma = 0$

For $\sigma = 0$, $l \neq 0$, $\kappa = 0$ we obtain to O(a), but with terms O($a\delta_R{}^2l^2$) neglected,

$$\phi = -i(\tau_0/l)(1 - e^{-rx}), \quad (3.20a)$$

$$g = i(\tau_0/l)e^{-rx}, \quad (3.20b)$$

and it follows that

$$\tilde{u}_1 = \tau_0(1 - e^{-rx}), \quad \tilde{v}_1 = i(\tau_0/l)re^{-rx}, \qquad (3.21a,b)$$

$$\tilde{u}_2 = \tilde{v}_2 = 0. \qquad (3.21c)$$

Consequently, for $\alpha \neq 0$, $l \neq 0$, a steady state exists that differs considerably from the frictionless steady solution (3.19). Here, to O(a) the lower-layer velocities u_2, $v_2 = 0$. All of the motion outside of the surface Ekman layer is confined to the upper layer within a frictionally modified Rossby radius r^{-1} of the coast.

4) RESONANCE, $\sigma = \omega_R$ $\alpha \neq 0$.

For $\sigma = \omega_R$, $\alpha \neq 0$, we obtain

$$C_1 = \frac{\tau_0}{la\alpha} \frac{(\omega_0^2 + \alpha^2)}{\frac{1}{2}\omega_0 + \alpha^2} [1 + O(a)]. \qquad (3.22)$$

Bottom friction thus limits the magnitude of the response of h for $l \neq 0$. For $(\sigma/\alpha)^2 \ll 1$ and

$$\sigma > \alpha^2 \{\sigma = \omega_0[1 + O(a)]\},$$

$|C_1|$ actually increases in magnitude as the friction coefficient α increases, in a manner related to the behavior of ω_I in (3.10b) and the accompanying decrease in magnitude of lower-layer velocities.

The limiting solutions found here for $\sigma \to 0$ would, of course, be modified at low enough frequencies by the β-effect (Anderson and Gill, 1975). At midlatitudes, however, these frequencies are relatively low. For example, in this model on an eastern ocean boundary, the baroclinic component remains trapped on a scale O(δ_R) for dimensional periods

$$T' \ll T'_T = 2(2\pi)(\beta'\delta'_R)^{-1}$$

(Allen and Romea, 1980). With $\beta' = 2 \times 10^{-13}$ cm^{-1} s^{-1} and $\delta'_R \approx 25$ km, $T'_T \approx 300$ days.

4. Weak slope

Here we model the continental shelf and slope topography with the weak-slope geometry (2.13) that supports shelf-wave solutions. With the weak slope, the frictional modifications to free and forced internal Kelvin waves are essentially the same as in the flat-bottom case discussed in Section 3. Therefore, we do not pursue that aspect of the problem here, but rather we concentrate on the modifications of the forced-shelf-wave response at midlatitudes due to the combined effects of stratification and bottom friction.

In addition to (2.13), we make assumptions (2.9), (2.11), (2.12), (2.14) and (2.15), i.e., that α, l_0, a, $\delta_R \ll 1$, and that $\tau^x = 0$, $\tau^y = \tau(y, t)$. The derivation of approximate equations and boundary conditions for shelf variables under these assumptions is discussed in Appendix A; they are

$$\psi_{xxt} + \delta_B^{-1}(\psi_y - h_y - \tau) + \alpha(\psi_{xx} - h_{xx}) = 0, \qquad (4.1a)$$

$$(h_{xx} - \delta_R^{-2}h)_t - a\delta_B^{-1}(\psi_y - h_y - \tau) - a\alpha(\psi_{xx} - h_{xx}) = 0, \qquad (4.1b)$$

$$\psi_y = 0 \text{ at } x = 0, \qquad (4.2a)$$

$$h_{xt} + h_y + a\alpha(h_x - \psi_x) = -\tau \quad \text{at} \quad x = 0, \qquad (4.2b)$$

$$\psi_x = 0, \quad h_x = -\delta_R^{-1}h \quad \text{at} \quad x = 1. \qquad (4.2c,d)$$

For $a \ll 1$, we obtain solutions to (4.1) and (4.2) by expanding in powers of a, i.e.,

$$h = h_0 + ah_1 + \cdots, \quad \psi = \psi_0 + a\psi_1 + \cdots. \qquad (4.3)$$

As mentioned above, we concentrate on the results for h_0 and ψ_0. The resulting problem for these variables is

$$(h_{0xx} - \delta_R^{-2}h_0)_t = 0, \qquad (4.4a)$$

$$\psi_{0xxt} + \delta_B^{-1}\psi_{0y} + \alpha\psi_{0xx} = \delta_B^{-1}(\tau + h_{0y}) + \alpha h_{0xx}, \qquad (4.4b)$$

$$\psi_{0y} = 0, \quad h_{0xt} + h_{0y} = -\tau \quad \text{at} \quad x = 0, \qquad (4.5a,b)$$

$$\psi_{0x} = 0, \quad h_{0x} = -\delta_R^{-1}h_0 \quad \text{at} \quad x = 1. \qquad (4.5c,d)$$

a. *Sinusoidal forcing*

With

$$\tau = \tau_0 \exp(i\sigma t + ily) \qquad (4.6)$$

$$(\psi_0, h_0) = (\phi, g) \exp(i\sigma t + ily), \qquad (4.7)$$

we obtain

$$g = Ce^{-rx}, \qquad (4.8a)$$

$$\phi = -(i\tau_0/l)(1 - \cosh px + \tanh p \sinh px) + CD(e^{-rx} - \cosh px + \tanh p \sinh px), \qquad (4.8b)$$

where

$$C = (i\tau_0/l)[1 - \sigma(l\delta_R)^{-1}]^{-1}, \qquad (4.8c)$$

$$D = (-p^2 + \hat{\alpha}\delta_R^{-2})/(-p^2 + \delta_R^{-2}), \qquad (4.8d)$$

$$r = \delta_R^{-1}, \quad p^2 = -il[\delta_B(i\sigma + \alpha)]^{-1}. \qquad (4.8e)$$

In particular, the contribution of ϕ to the alongshore velocity is

$$\phi_x = Ep[-\sinh px + \tanh p \cosh px] - CD\delta_R^{-1}e^{-rx}, \qquad (4.9a)$$

where

$$E = -(i\tau_0/l) + CD. \qquad (4.9b)$$

For the case of a barotropic fluid with no stratification ($C = 0$), the remaining nonzero parts of ϕ and ϕ_x represent the forced-shelf-wave response. In that case, with no friction ($\alpha = 0$)

$$p = p_1 = [-l/(\delta_B\sigma)]^{1/2}, \qquad (4.10)$$

and resonance with long barotropic-shelf-wave modes exists for values of l and σ such that $l/\sigma > 0$ and $\cos p_1 = 0$. For $\alpha \neq 0$ and $\sigma = 0$,

$$p = p_2 = \exp\left(i\frac{3}{4}\pi\right)\delta_F^{-1}, \quad \delta_F = (\alpha\delta_B/l)^{1/2}, \quad (4.11)$$

and the resultant barotropic steady state solution for ϕ and ϕ_x corresponds to the "arrested topographic wave" (Csanady, 1978) for this geometry (see Appendix C).

In the stratified case ($C \neq 0$) the behavior of ϕ_x in the steady state limit $\sigma \to 0$ will be of interest. We will refer to that part of ϕ_x multiplied by E on the right-hand side of (4.9a) as the forced-shelf-wave response. For $x \gg r^{-1}$, the velocity field below the surface Ekman layer is due solely to this component and is barotropic.

First, with no friction ($\alpha = 0$) we find

$$C \sim (i\tau_0/l)[1 + \sigma(l\delta_R)^{-1} + \cdots], \quad (4.12a)$$

$$CD \sim (i\tau_0/l)[1 - \sigma(l\delta_R)^{-1}(\delta_B\delta_R^{-1} - 1) + \cdots], \quad (4.12b)$$

$$E \sim -(i\tau_0/l)\sigma(l\delta_R)^{-1}(\delta_B\delta_R^{-1} - 1). \quad (4.12c)$$

As $\sigma \to 0$, (4.4b) requires that $\psi_{0y} - h_{0y} - \tau \sim 0$, i.e., that the lower-layer cross-shelf velocity vanish, and (4.12) shows that the magnitude of the forced-shelf-wave solution $E \sim 0$ and that $CD \sim C \sim i\tau_0/l$. As a consequence, both lower-layer velocities u_2, $v_2 \sim 0$ and the motion is confined to the upper layer within δ_R of the coast in agreement with the results of Romea and Allen (1982).

With friction ($\alpha \neq 0$) in the limit $\sigma \to 0$, C is again given by (4.12a), while

$$CD \sim (i\tau_0/l)[1 + \sigma(l\delta_R)^{-1} - i(\sigma/\alpha)(1 - i\delta_R{}^2\delta_F{}^{-2})^{-1} + \cdots], \quad (4.13a)$$

$$E \sim (i\tau_0/l)\sigma(l\delta_R)^{-1}[1 - i\delta_R\delta_B\delta_F{}^{-2} \times (1 - i\delta_R{}^2\delta_F{}^{-2})^{-1} + \cdots]. \quad (4.13b)$$

Thus, as $\sigma \to 0$, again $E \sim 0$, $CD \sim C \sim (i\tau_0/l)$, and u_2, $v_2 \sim 0$. If $\sigma/\alpha \ll 1$, the approach as $\sigma \to 0$ of the lower-layer velocities to zero is faster with friction, however. This comes about because, with the assumptions that $\delta_R\delta_B = O(1)$ and $\delta_F = O(1)$, CD and E approach their asymptotic values as $\sigma(l\delta_R)^{-1} \to 0$ (and $\sigma/\alpha \to 0$), whereas without friction the asymptotic values are approached as the larger quantity $(\delta_B/\delta_R)[\sigma(l\delta_R)^{-1}] \to 0$. It is worthy of note here that since E, the coefficient of the forced-shelf-wave response, goes to zero as $\sigma \to 0$, the "arrested topographic wave" which forms the steady solution in the barotropic case has zero magnitude and plays no role in the steady stratified solution.

b. *First-order wave equations*

The way in which the qualitative features of the forced response, found with sinusoidal forcing in Section 4a, develop in more general problems can be shown most easily by deriving and solving equations for the alongshore and time-dependent behavior of cross-shelf modes.

We again consider equations (4.4), with boundary conditions (4.5), and write h_0 and ψ_0 as

$$h_0 = Y_0(y, t), e^{-rx}, \quad (4.14)$$

$$\psi_0 = \hat{\psi}_0(x, y, t) + Y_p(y, t)(e^{-rx} - 1), \quad (4.15)$$

where $r = \delta_R^{-1}$ and

$$-\delta_R^{-1}Y_{0t} + Y_{0y} = -\tau(y, t), \quad (4.16)$$

$$Y_{pt} = \alpha(Y_0 - Y_p), \quad (4.17)$$

$$\hat{\psi}_{0xxt} + \delta_B^{-1}\hat{\psi}_{0y} + \alpha\hat{\psi}_{0xx} = \delta_B^{-1}(\tau + Y_{py}) + \delta_B^{-1}(Y_{0y} - Y_{py})e^{-rx}, \quad (4.18)$$

and where

$$\hat{\psi}_{0y} = 0 \quad \text{at} \quad x = 0, \quad (4.19a)$$

$$\hat{\psi}_{0x} = 0 \quad \text{at} \quad x = 1. \quad (4.19b)$$

The variable Y_0 may be found from (4.16) and then Y_p may be obtained from (4.17). These terms then act, along with τ, as forcing functions in (4.18), which has the same form as a forced-shelf-wave problem. Accordingly, it is convenient to expand $\hat{\psi}_0$ in terms of inviscid cross-shelf modes, as done by Gill and Schumann (1974):

$$\hat{\psi}_0 = \sum_{n=1}^{\infty} Y_n(y, t)\phi_n(x), \quad (4.20)$$

which gives

$$-c_n^{-1}Y_{nt} + Y_{ny} - \alpha c_n^{-1}Y_n = (\tau + Y_{py})b_n + (Y_{0y} - Y_{py})d_n, \quad (4.21)$$

where

$$\phi_{nxx} + \kappa_n{}^2\phi_n = 0, \quad \phi_n(0) = \phi_{nx}(1) = 0, \quad (4.22a,b)$$

$$\phi_n = \sqrt{2}\sin\kappa_n x, \quad (4.22c)$$

$$\kappa_n = (2n - 1)\frac{1}{2}\pi, \quad n = 1, 2, 3, \ldots, \quad (4.22d)$$

$$1 = \sum_{n=1}^{\infty} b_n\phi_n, \quad e^{-rx} = \sum_{n=1}^{\infty} d_n\phi_n, \quad (4.23a,b)$$

$$b_n = \sqrt{2}/\kappa_n, \quad d_n = \sqrt{2}\kappa_n/(r^2 + \kappa_n{}^2), \quad (4.23c,d)$$

$$c_n = (\delta_B\kappa_n{}^2)^{-1}. \quad (4.24)$$

To illustrate the nature of the response, we choose a simple three-dimensional, initial-value problem with

$$\tau = \tau_0\hat{H}(-y)\hat{H}(t), \quad (4.25)$$

where $\hat{H}$ is the Heaviside unit function and where $h = \psi = 0$ for $t < 0$. We therefore seek the solutions to (4.16), (4.17) and (4.21) with τ given by (4.25) and with

$$Y_0 = Y_p = Y_n = 0, \quad t < 0. \quad (4.26)$$

Before proceeding with the stratified problem, it is useful to consider the response to (4.25) in the purely barotropic case governed by (4.21) with $Y_0 = Y_p = 0$. We obtain:

In region A, $t \leqslant -y/c_n$:

$$Y_n = -c_n b_n \tau_0 \alpha^{-1}(1 - e^{-\alpha t}). \quad (4.27a)$$

In region B, $t \geqslant -y/c_n$:

$$Y_n = -c_n b_n \tau_0 \alpha^{-1}[1 - \exp(\alpha y/c_n)]. \quad (4.27b)$$

For $\alpha t \gg 1$, $Y_n \sim -c_n b_n \tau_0 \alpha^{-1}$ in A, so that Y_n is steady for all y. It has the y-structure plotted in Fig. 2 and it forms the contribution of the nth mode to the "arrested topographic wave" steady solution (Appendix C).

For the stratified problem, we find:

In region 1, $t \leqslant -y/\delta_R$:

$$Y_0 = \tau_0 \delta_R t, \quad (4.28a)$$

$$Y_p = \tau_0 \delta_R [t - \alpha^{-1}(1 - e^{-\alpha t})]. \quad (4.28b)$$

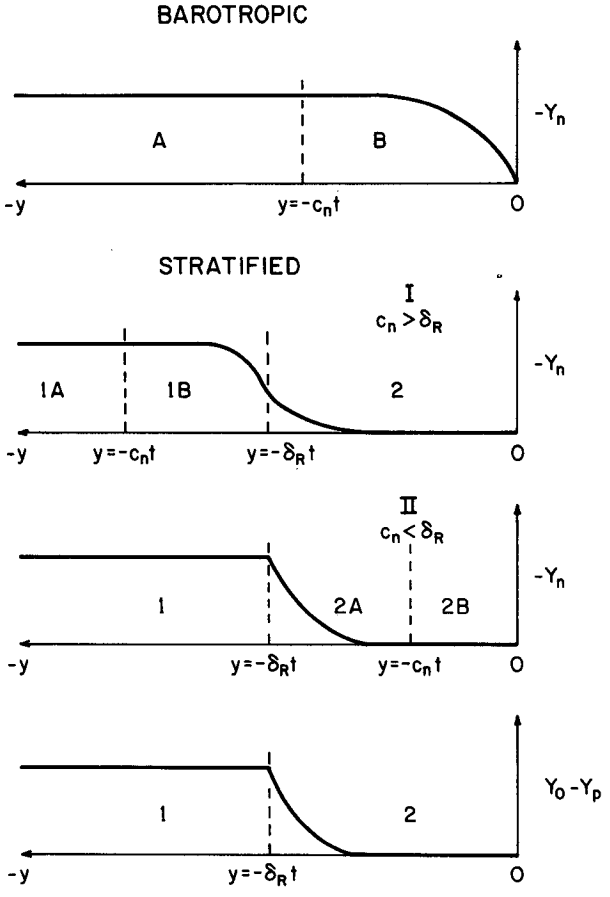

FIG. 2. Schematic of Y_n for $\alpha t \gg 1$ for (from the top) the barotropic case (4.27), stratified Case I ($c_n > \delta_R$) Case II ($c_n < \delta_R$) (4.29) and a schematic of $Y_0 - Y_p$ for $\alpha t \gg 1$ (4.28).

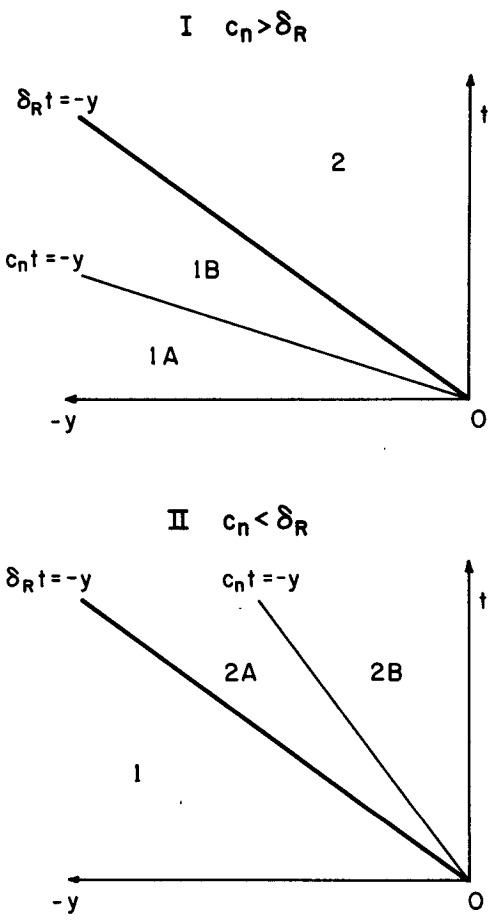

FIG. 3. Diagrams of y–t for the solutions (4.28) and (4.29) in stratified Case I ($c_n > \delta_R$) and Case II ($c_n < \delta_R$).

In region 2, $t \geqslant -y/\delta_R$:

$$Y_0 = -\tau_0 y, \quad (4.28c)$$

$$Y_0 = -\tau_0[y + \alpha^{-1}\delta_R(e^{-\alpha(t+y\delta_R^{-1})} - e^{-\alpha t})]. \quad (4.28d)$$

The resulting solution for Y_n differs depending on whether (Case I) $c_n > \delta_R$ or (Case II) $c_n < \delta_R$ (see Figs. 2 and 3):

CASE I, $c_n > \delta_R$

In 1A, $-y/c_n \geqslant t \geqslant 0$:

$$Y_n = -\tau_0 \alpha^{-1} c_n b_n (1 - e^{-\alpha t}). \quad (4.29a)$$

In 1B, $-y/\delta_R \geqslant t \geqslant -y/c_n$:

$$Y_n = -\tau_0 \alpha^{-1}\langle c_n b_n \{1 - \exp[\alpha(y + \delta_R t)(c_n - \delta_R)^{-1}]\} + \delta_R(b_n - d_n)\{\exp[\alpha(y + \delta_R t) \times (c_n - \delta_R)^{-1}] - \exp(-\alpha t)\}\rangle. \quad (4.29b)$$

In 2, $t \geqslant -y/\delta_R$:

$$Y_n = -\tau_0 \alpha^{-1}\delta_R(b_n - d_n) \times \{\exp[-\alpha(t + y\delta_R^{-1})] - \exp(-\alpha t)\}. \quad (4.29c)$$

CASE II, $c_n < \delta_R$

In 1, $-y/\delta_R \geq t \geq 0$: (4.29a).

In 2A, $-y/c_n > t \geq -y/\delta_R$:

$$Y_n = -\tau_0\alpha^{-1}\{\delta_R(b_n - d_n)\exp[-\alpha(t + y\delta_R^{-1})] + [b_nc_n - \delta_R(b_n - d_n)]\exp[\alpha(y + \delta_R t) \times (c_n - \delta_R)^{-1}] - b_nc_n\exp(-\alpha t)\}. \quad (4.29d)$$

In 2B, $t \geq -y/c_n$: (4.29c).

In the limit of no friction, $\alpha = 0$, $Y_p = 0$ and (4.29) gives

CASE I, $c_n > \delta_R$

In 1A: $$Y_n = -\tau_0 b_n c_n t. \quad (4.30a)$$

In 1B: $$Y_n = \tau_0 b_n y - \tau_0\delta_R d_n(y + c_n t)(\delta_R - c_n)^{-1}. \quad (4.30b)$$

In 2: $$Y_n = \tau_0(b_n - d_n)y. \quad (4.30c)$$

CASE II, $c_n < \delta_R$

In 1: (4.30a).

In 2A: $$Y_n = -\tau_0 b_n c_n t + \tau_0 d_n c_n(y + \delta_R t)(\delta_R - c_n)^{-1}. \quad (4.30d)$$

In 2B: (4.30c).

For fixed negative y and large time, i.e., in region 2 (Case I, $c_n > \delta_R$) and region 2B (Case II, $c_n < \delta_R$), Y_n is steady. When all the modes have achieved this steady state,

$$\psi_0 = \hat{\psi}_0 = \tau_0 y \sum_n (b_n - d_n)\phi_n = \tau_0 y(1 - e^{-rx})$$

which together with $h = -\tau_0 y e^{-rx}$ implies

$$u_1 = \tau_0(1 - e^{-rx}), \quad (4.31a)$$

$$v_1 = -(\tau_0 y/\delta_R)e^{-rx}, \quad (4.31b)$$

$$u_2 = v_2 = 0. \quad (4.31c)$$

The resulting currents outside the surface Ekman layer are confined to the upper layer within δ_R of the coast, similar to the results for $\alpha = 0$, $\sigma \to 0$ in Section 4a and as found by Romea and Allen (1982) for the inviscid case. The steady currents in the upper layer provide (receive) the offshore (onshore) Ekman transport. Thus, for $y < 0$, u_1 is independent of y while v_1 varies linearly with y. Since d_n is a maximum for $\kappa_n^2 = \delta_R^{-2}$, which implies $c_n = \delta_R^2/\delta_B$, the adjustment to the steady limit necessarily involves the modes for which $c_n \ll \delta_R$.

The frictionless steady limit with bottom slope may be contrasted to the frictionless steady limit with a flat bottom where the solution is given by Y_0 alone and where for $t \geq -y/\delta_R$,

$$u_1 = H_2\tau_0(1 - e^{-rx}), \quad (4.32a)$$

$$v_1 = -H_2(\tau_0 y/\delta_R)e^{-rx}, \quad (4.32b)$$

$$u_2 = -au_1, \quad v_2 = -av_1. \quad (4.32c,d)$$

The alongshore current system is confined to $y < 0$ and a region of $O(\delta_R)$ from the coast, but it involves oppositely directed velocities in the upper and lower layers, with the lower-layer alongshore velocity forming an undercurrent.

With friction ($\alpha \neq 0$) the limiting values of Y_p and Y_n for $\alpha t \gg 1$ are obtained from (4.28) and (4.29) by neglecting the $\exp(-\alpha t)$ terms. Plots of Y_n and of $(Y_0 - Y_p)$ as a function of y for $\alpha t \gg 1$ are also shown in Fig. 2.

For $\alpha t \gg 1$, in region 1 $Y_0 - Y_p \sim \tau_0\alpha^{-1}\delta_R$. In regions 1A (Case I) and 1 (Case II), $Y_n \sim -\tau_0\alpha^{-1}c_nb_n$, representing the solution of $\alpha\hat{\psi}_{0xx} = \delta_B^{-1}\tau$. The corresponding velocity components are

$$v_1 = H_2\tau_0 t e^{-rx}[1 + O(a)], \quad (4.33a)$$

$$v_2 = -H_1\tau_0\alpha^{-1}[e^{-rx} - \delta_B^{-1}(1 - x)]. \quad (4.33b)$$

Thus, v_1 increases linearly with t whereas v_2 is steady. Within δ_R of the coast, v_1 and v_2 are opposite in direction so that an undercurrent is present.

Also, for $\alpha t \gg 1$, Y_n reaches a state that is steady with respect to the coordinate $\eta = y + \delta_R t$. A "modified arrested topographic wave" solution exists in region 1, $-y \geq \delta_R t$, with an exponential decay on scale $\delta_2 = \delta_R/\alpha$ into region 2, $-y \leq \delta_R t$. Outside of this exponential tail in region 2, i.e., for $-y \ll \delta_2 + \delta_R t$, $Y_n \sim 0$. Thus, in contrast to the purely barotropic case shown in Fig. 2, for $\alpha t \gg 1$ the modified "arrested topographic wave" here essentially only exists for $-y \geq \delta_R t + \delta_2$ and it propagates steadily alongshore in the negative y-direction at the internal Kelvin wave speed δ_R. In a sense, the effects of stratification liberate the "arrested topographic wave," allowing it to propagate steadily toward negative y. In terms of the coordinate $\eta = y + \delta_R t$, the liberated or "modified arrested topographic wave" satisfies

$$\delta_R\hat{\psi}_{0xx\eta} + \delta_B^{-1}\hat{\psi}_{0\eta} + \alpha\hat{\psi}_{0xx} = R, \quad (4.34a)$$

where

$$R = \begin{cases} \delta_B^{-1}\tau_0 & \text{for } \eta < 0, \quad (4.34b) \\ \delta_B^{-1}\tau_0(1 - e^{-rx})e^{-\alpha\eta} & \text{for } \eta > 0. \quad (4.34c) \end{cases}$$

In the part of region 2 where $Y_n \sim 0$, i.e., for $-y \ll \delta_2 + \delta_R t$, we also find $Y_p - Y_0 \sim 0$. The resulting velocity components are given by (4.31) and again the steady currents outside the surface Ekman layer are confined to the upper layer within δ_R of the coast.

The effects of both bottom friction and bottom slope individually lead to the same current system with lower-layer velocities equal to zero and no undercurrent present. The development with friction is more rapid in the sense that for $\alpha t \gg 1$, the limiting steady state at a given y is reached after a time

$t > \delta_R^{-1}(-y + \delta_2)$, whereas in the frictionless case with bottom slope the time would be $t > -c_n^{-1}y$, where $c_n \ll \delta_R$. Assuming that this process occurs at an eastern ocean boundary, the β-effect would allow, on a longer time scale, the steady current found here to propagate into the interior as baroclinic Rossby waves (Anderson and Gill, 1975).

5. Discussion

The main qualitative result of interest found in the preceding analysis is the decrease of velocities in the lower layer and the resultant concentration of currents in the upper layer within a Rossby radius of the coast as the frequency of motion with alongshore gradients approaches zero.

This is found for the free internal Kelvin waves in Section 3a, where, for $\omega_0/\alpha \to 0$, the magnitude of the velocity components in the lower layer that vary in x on the Rossby-radius scale approach zero. In addition, the imaginary component of the frequency in (3.10b) asymptotes for $(\omega_0/\alpha)^2 \ll 1$ to $\omega_I \approx \omega_0 a[\frac{1}{2}(\omega_0/\alpha) + \alpha]$, so that the decay time scale T_F of the free-wave amplitude due to bottom friction is a function of frequency and it decreases and vanishes as $\omega_0 \to 0$. Specifically, for waves of period T, as $\omega_0 \to 0$, $T_F \approx T(2\pi a\alpha)^{-1}$. Consequently, coastal internal Kelvin waves may be able to participate with relatively small damping by bottom friction in low-frequency phenomena such as El Niño. It is also worth noting that bottom friction decreases the free-wave speed, with the largest decrease found at low frequencies.

In the analysis by Brink (1982), on the effect of bottom friction on free coastal-trapped waves in a stratified ocean, the range of the free-wave frequency is limited in order to preserve the validity of the perturbation method employed. In the present model, that range of validity corresponds to $\alpha/\omega_0 \ll 1$. Thus, the effective ω_I found in that paper corresponds to the constant value $\omega_I \approx \frac{1}{2}a\alpha$ in (3.9b). Although that model is more realistic in other respects, the analysis procedure utilized does not apply for $(\omega_0/\alpha)^2 \ll 1$ and consequently does not reveal the upper-layer concentration of velocity and decrease in frictional decay found in (3.10) and (3.11).

The effect of friction on free internal Kelvin waves, with continuous and two-layer stratification, has also been investigated by Martinsen and Weber (1981). In the continuously stratified case, internal friction was included, but the bottom stress was taken equal to zero. This represents a situation different from that studied here. In the two-layer model, both interface and bottom friction were included, but the contribution from bottom friction was eventually neglected. Additionally, in the formulation it was assumed that the baroclinic mode was uncoupled from the barotropic mode. As shown clearly by Eqs. (3.1), with bottom friction that assumption is incorrect in general. In any case, their results do not correspond to those found here.

In the forced problems, where τ^y has alongshore variability, e.g., with $l \neq 0$ in Sections 3b and 4a or with $\tau = \tau_0\hat{H}(-y)\hat{H}(t)$ in Section 4b, a result similar to the free-wave case is obtained. As the forcing frequency $\sigma \to 0$ or as a steady state is approached for fixed y ($-y < \delta_R t + \delta_2$) in Section 4b, the lower-layer velocities $u_2, v_2 \sim 0$ and the currents are confined to the upper layer within a region $O(\delta_R)$ from the coast. In the weak-slope model, as the steady limit is approached the magnitude of the forced-shelf-wave component of the solution asymptotes to zero. As a result, the barotropic "arrested topographic wave" plays no role in these stratified steady state solutions.

Pedlosky (1974a) examined the effect of bottom friction on the coastal response to wind stress of a continuously stratified fluid in a weak-slope, channel model. The forcing utilized was similar to that in Section 4b. The analysis was completed under the assumption that the baroclinic component of the response (in the hydrostatic layer there) remained in a two-dimensional unsteady balance. The forced barotropic component (in the topographic layer) was unaffected by the time development of the baroclinic component. In the problem in Section 4b, corresponding assumptions and results would be valid for $t \leqslant -y/\delta_R$ and $t \leqslant -y/c_n$, i.e., for Case I in region 1A and Case II in region 1. Although the present two-layer model is more idealized than that of Pedlosky (1974a), the simplifications here allow approximate solutions to be easily obtained for all regions of the y–t plane. That is not readily done with the continuously stratified model. In particular, the response in region 2, $t \geqslant -y/\delta_R$ or its analog, where we found that the magnitude of the barotropic "arrested topographic wave" component approaches zero for $-y \ll \delta_R t + \delta_2$, was not investigated by Pedlosky (1974a).

It should be pointed out that the steady forced solutions obtained with this two-layer model do not have a direct correspondence in the linear continuously stratified case. The equation for the density in linear, nondiffusive, continuously stratified models is approximated by $\rho_t + w\bar{\rho}_z = 0$, where $\bar{\rho}_z = \bar{\rho}_z(z)$ is the mean vertical density gradient. With bottom friction, the same equation holds so that an absolute steady state would require $w = 0$. A steady state with $w \neq 0$, needed in any finite-depth current to match the Ekman-suction condition at the coastal corner, cannot exist without other processes such as dissipation or nonlinearities playing a role. These processes would most likely involve small vertical scales and affect the higher vertical modes. Questions about the behavior on these scales are not addressed in the two-layer approximation.

The fact that the "arrested topographic wave" component of the flow vanishes in the steady state solutions found here is of interest. Because of the idealized nature of the present model, we do not want to emphasize this point unduly. Nonetheless, the vanishing of the forced-shelf-wave component accompanies the upper-layer concentration of velocities; this general feature may well be important for stratified shelf flow fields, especially on long time scales of several weeks to several months. Enfield and Allen (1980) made an attempt to investigate the possible quasi-steady balance at the coast of

$$\int_{y_1}^{y_2} \tau^y dy = p_1(y_2) - p_1(y_1)$$

on a several-month time scale using coastal sea-level and wind-stress data. Whether such a basic balance, representing, in terms of alongshore averages, a geostrophic onshore (offshore) velocity providing transport equal to the offshore (onshore) Ekman transport, should be expected is not known based on existing coastal models. That balance is achieved as $\sigma \to 0$ in (3.21) and (4.12a). However, results for a barotropic fluid (Csanady, 1978), with bottom friction and a more realistic wedge geometry at the coast, imply a different balance, $\tau = \alpha p_x$, at the coast. Clearly, a frictional, stratified model with realistic cross-shelf topography and realistic stratification is needed to answer that question. The results found here, however, give an indication of general flow-field characteristics to expect, and they cast doubt on the ability of barotropic models to explain low-frequency behavior in stratified coastal regions. In fact, several qualitative features exhibited by existing current measurements agree with those predicted here, as discussed below.

Some of the behavior found for the alongshore velocity field in the forced examples in Sections 3b and 4 is similar to qualitative features of observed currents on the Oregon shelf. In Fig. 4, we show the vertical structure of the mean and the fluctuating components of the alongshore currents at midshelf in a water depth of about 100 m for a summer period and a winter period of approximately two months each (redrawn from Huyer *et al.*, 1978). In the summer, the fluctuating component is nearly depth-independent whereas the two-month mean has considerable vertical shear evidently associated with an inviscid thermal-wind balance. The fluctuations appear to be barotropic at this midshelf location but exhibit larger vertical shear at an inshore mooring. In contrast, the reason why the mean-flow component is so highly baroclinic has never really been explained. This behavior is consistent with the results in Sections 3b and 4a, where, as the forcing frequency decreases, i.e., as σ/α and $\sigma/(l\delta_R)$ decrease, the barotropic forced-shelf-wave component decreases in magnitude and the offshore scale r^{-1} of the baroclinic component

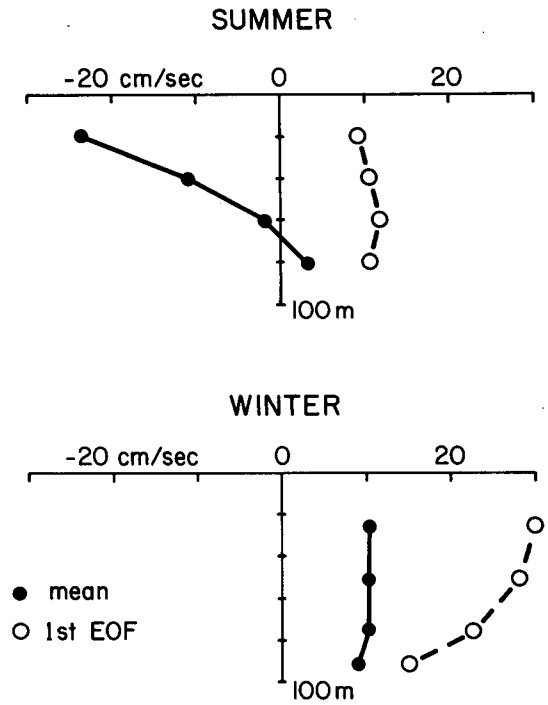

FIG. 4. Mean values of the alongshore velocity and scaled alongshore components of the first empirical orthogonal function (EOF) from midshelf locations (water depth ~ 100 m) on the Oregon shelf for summer (2 July–26 August 1973) and winter (1 February–24 March 1975) (redrawn from Huyer *et al.*, 1978). The EOFs have been calculated from the low-passed (40 h half-power point) observations of horizontal velocity vectors for the set of depths shown. The first EOF accounts for 85% of the variance in the summer and 93% in winter. The normalized components of the EOF have been scaled by the standard deviation of the modal amplitude.

(3.6b) increases. The magnitude of the baroclinic shear within r^{-1} depends in (4.12a) on (τ_0/l), and it is reasonable that representative values for this coefficient increase as σ decreases.

In the winter, the fluctuations are larger in magnitude and have a great deal more vertical shear than those in the summer. The vertical shear in the fluctuations is reported to be inviscidly balanced by cross-shelf gradients of density, consistent with the thermal wind relation (Huyer *et al.*, 1978). The reason for this change in structure of the fluctuations between summer and winter also has not been explained. If the effective value of α is determined by a nonlinear drag law, then the increased magnitude of the fluctuations in the winter could lead to larger values for α. In addition, an increase in amplitude of the surface-wave field in the winter may lead to larger values of bottom stress (Grant and Madsen, 1979) and thus contribute to increasing the effective value of α. An increase in vertical shear of the wind-stress-forced, fluctuating alongshore velocity components with an increase in α is found here in two different examples. In the results from the purely two-dimen-

sional cases (3.16) and (B9), as the friction coefficient α is increased with fixed values of the forcing frequency, the magnitude of the lower-layer alongshore velocity decreases while the magnitude of the upper-layer alongshore velocity is unaffected, thus increasing the vertical shear. In the resonant response of forced internal Kelvin waves (3.22), the magnitude of the baroclinic component $|C_1|$ increases as α increases if the forcing frequency α is in the range $(\sigma/\alpha)^2 \ll 1$ and $\frac{1}{2}\sigma > \alpha^2$. The magnitude of the vertical shear, of course, increases with $|C_1|$.

Figure 4 also shows that the mean velocities in the winter have less vertical shear than those in the summer, as well as having opposite sign. The difference in the shear is presumably not related to the present model results, but is associated with a change in vertical position of the seasonal mean pycnocline (Huyer *et al.*, 1978).

The weak-slope, two-layer model is admittedly highly idealized. The representation at midlatitudes of a coastal boundary by a vertical wall may lead to misleading results. The importance for real shelf flow fields of the physics found within the internal Rossby radius in weak-slope, vertical-coast models is not clear, as we have discussed elsewhere (Allen, 1980). In addition, the representation of the effects of stratification by two layers leaves out features of interest associated with continuous stratification. Nevertheless, in spite of the model shortcomings, the primary result found here, that for three-dimensional stratified coastal flow the current field tends to weaken in the bottom layer and to concentrate in the upper layer as the frequency of the motion decreases, seems to represent basic behavior that is evidently present in observations and is likely to appear in more complex models.

Acknowledgments. This research was supported by the Oceanography Section of the National Science Foundation under Grants OCE-7826820, OCE-8026131 and OCE-8014939 (Coastal Ocean Dynamics Experiment). The author thanks an anonymous referee and Dr. K. H. Brink for constructive comments.

APPENDIX A

Approximate Equations for the Shelf and Slope

The derivation of approximate equations governing the motion on the continental shelf and slope under assumptions (2.3), (2.9), (2.11) and (2.13) is discussed below. The procedure is similar to that of Romea and Allen (1982) (see also Allen, 1976) for the frictionless case. Since the addition of bottom-friction effects is straightforward, the derivation is simply outlined.

The governing equations are (2.7), which were derived from (2.1) with the assumption $\delta_t \gg 1$ (2.3), and with $H = H(x)$. The bottom stresses in (2.7) are given by (2.8a, b) and (2.10) with assumption (2.9).

The basic assumption for the coastal region is $2\pi/\delta_y = l_0 \ll 1$ (2.11), i.e., that onshore–offshore scales, set either by the shelf-slope width or the Rossby radius of deformation δ_R, are much smaller than alongshore scales δ_y. The motion in the interior, off the shelf and slope, is assumed to vary on large x- and y-scales of $O(\delta_y)$, although adjacent to the slope there may be a component that varies on an x-scale of $O(\delta_R)$. A systematic derivation of approximate equations under (2.13) is facilitated by rescaling the coordinates to reflect the above assumptions (e.g., Romea and Allen, 1982). For simplicity in notation here, however, we will record all equations in terms of the original dimensionless variables defined in Section 2.

As a result of assumption (2.11), the approximate equations governing the variables on the shelf are

$$(\psi_{xx} - \delta_B^{-1}\psi_x)_t + \delta_B^{-1}(\psi_y - h_y - \tau^y_{(0)}) - \alpha H[(-\psi_x + h_x)H^{-2}]_x = 0, \quad \text{(A1a)}$$

$$(h_{xx} + a\delta_B^{-1}h - \delta_R^{-2}h)_t - a\delta_B^{-1}(\psi_y - h_y - \tau^y_{(0)}) + a\alpha H[(-\psi_x + h_x)H^{-2}]_x = 0, \quad \text{(A1b)}$$

where we use the notation $\tau^y_{(0)} = \tau^y$ $(x = 0)$. The boundary conditions at the coast follow from the requirement that $u_1 = u_2 = 0$ and are

$$\psi_y = 0 \quad \text{at} \quad x = 0, \quad \text{(A2a)}$$

$$h_{xt} + h_y + a(\alpha/H)(-\psi_x + h_x) = -\tau^y_{(0)} \quad \text{at} \quad x = 0. \quad \text{(A2b)}$$

The alongshore velocity components v_1, v_2 on the shelf are given by (2.6b, d) with the terms in square brackets in (2.6f) neglected. As a result, the alongshore velocity is assumed to be in geostrophic balance.

The variables in the interior, off the shelf and slope, are conveniently written as the sum of two terms:

$$\psi = \psi_I + \psi_B, \quad h = h_I + h_B, \quad \text{(A3a,b)}$$

where ψ_I, h_I vary on large x- and y-scales of $O(\delta_y)$, while ψ_B, h_B vary on an x-scale of $O(\delta_R) = O(1)$. The approximate equations governing these variables are

$$\nabla^2\psi_{It} + \alpha\nabla^2(\psi_I - h_I) - \alpha(\tau_y{}^y + \tau_x{}^x) = \tau_y{}^x - \tau_x{}^y, \quad \text{(A4a)}$$

$$-\delta_R^{-2}h_{It} - a\alpha\nabla^2(\psi_I - h_I) + a\alpha(\tau_y{}^y + \tau_x{}^x) = \tau_y{}^x - \tau_x{}^y, \quad \text{(A4b)}$$

$$\psi_{Bxxt} + \alpha(\psi_{Bxx} - h_{Bxx}) = 0, \quad \text{(A4c)}$$

$$(h_{Bxx} - \delta_R^{-2}h_B)_t - a\alpha(\psi_{Bxx} - h_{Bxx}) = 0, \quad \text{(A4d)}$$

where $\nabla^2\phi = \phi_{xx} + \phi_{yy}$.

For simplicity here we assume that in the interior, (2.12) holds, i.e.,

$$a \ll 1.$$

It follows from (A4c, d) that

$$(\psi_B, h_B) = (Y_p, Y_0)\exp(-x/\delta_R)[1 + O(a)], \quad \text{(A5a)}$$

$$Y_{pt} + \alpha Y_p = \alpha Y_0. \quad \text{(A5b)}$$

The matching conditions between the lowest-order shelf and interior variables, derived as a consequence of (2.11) (Allen, 1976; Romea and Allen, 1982), are

$$\psi_I(x = 0) = 0, \quad \text{(A6a)}$$

$$\psi_{xt}(x = 1) = \psi_{Bxt}(x = 1) + \psi_{Ixt}(x = 0), \quad \text{(A6b)}$$

$$h(x = 1) = h_B(x = 1) + h_I(x = 0), \quad \text{(A6c)}$$

$$h_x(x = 1) = h_{Bx}(x = 1), \quad \text{(A6d)}$$

where, because of the present notation, it is helpful to recall that ψ_I, h_I vary on a larger x-scale than ψ, h or ψ_B, h_B.

To solve the shelf problem, it is useful to define new variables

$$\psi = \hat{\psi} + \psi_{Ix(0)}\int_0^x H(\xi)d\xi, \quad \text{(A7a)}$$

$$h = \hat{h} + h_{I(0)}, \quad \text{(A7b)}$$

such that

$$(\hat{\psi}_{xx} - \delta_B^{-1}\hat{\psi}_x)_t + \delta_B^{-1}(\hat{\psi}_y - \hat{h}_y) - \alpha H[(-\hat{\psi}_x + \hat{h}_x)H^{-2}]_x = \delta_B^{-1}F_1, \quad \text{(A8a)}$$

$$(\hat{h}_{xx} + a\delta_B^{-1}\hat{h}_x - \delta_R^{-2}\hat{h})_t - a\delta_B^{-1}(\hat{\psi}_y - \hat{h}_y) + a\alpha H[(-\hat{\psi}_x + \hat{h}_x)H^{-2}]_x = -a\delta_B^{-1}F_1, \quad \text{(A8b)}$$

where

$$F_1 = \tau^y_{(0)} + h_{I(0)y} - \psi_{Ix(0)y}\int_0^x H(\xi)d\xi + \alpha\psi_{Ix(0)}. \quad \text{(A8c)}$$

The boundary conditions on $\hat{\psi}$ and $\hat{h}$ are

$$\hat{\psi}_y = 0 \quad \text{at} \quad x = 0, \quad \text{(A9a)}$$

$$\hat{h}_y + \hat{h}_{xt} + a(\alpha/H)(-\hat{\psi}_x + \hat{h}_x) = -F_2 \quad \text{at} \quad x = 0, \quad \text{(A9b)}$$

$$\hat{\psi}_x = \psi_{Bx} \quad \text{at} \quad x = 1, \quad \text{(A9c)}$$

$$\delta_R\hat{h}_x = -\hat{h} = -h_B \quad \text{at} \quad x = 1, \quad \text{(A9d)}$$

where, with assumption (2.12), ψ_B and h_B are obtained from (A5) and

$$F_2 = \tau^y_{(0)} + h_{I(0)y} - a\alpha\psi_{Ix(0)}. \quad \text{(A9e)}$$

For $\delta_R \ll 1$ [assumption (2.14)], $\psi_{Bx}(x = 1) = 0$ in (A9c).

Under the "weak-slope" approximation (2.13), i.e., $\delta_B^{-1} \ll 1$, Eqs. (A8) become

$$\hat{\psi}_{xxt} + \delta_B^{-1}(\hat{\psi}_y - \hat{h}_y) + \alpha(\hat{\psi}_{xx} - \hat{h}_{xx}) = \delta_B^{-1}F_1, \quad \text{(A10a)}$$

$$(\hat{h}_{xx} - \delta_R^{-2}h)_t - a\delta_B^{-1}(\hat{\psi}_y - \hat{h}_y) - a\alpha(\hat{\psi}_{xx} - \hat{h}_{xx}) = -a\delta_B^{-1}F_1, \quad \text{(A10b)}$$

where a, δ_B, δ_R and H are regarded as constants ($H = 1$) and where an additional, implicit assumption is that $\delta_B \gg a\delta_R$. The boundary conditions are given by (A9) where $H = 1$ in (A9b).

The above formulation, with interior variables incorporated in the forcing functions F_1 and F_2, is especially useful to have when the weak-slope approximation is utilized. That can be demonstrated in the simplified case where the motion is barotropic, frictionless and two-dimensional ($\partial/\partial y \equiv 0$), with $\tau^x = 0$ and $\tau^y = \tau^y(t)$. The exact solution, without the weak-slope approximation, is

$$\psi_{xt} = -\tau. \quad \text{(A11)}$$

This result is also obtained from (A7) and (A8) where, with

$$\psi_{Ix(0)t} = -\tau, \quad \text{(A12)}$$

we find

$$\hat{\psi}_{xt} = -\tau(1 - H), \quad \text{(A13a)}$$

$$\psi_{xt} = \hat{\psi}_{xt} + H\psi_{Ix(0)t} = -\tau. \quad \text{(A13b)}$$

Note that for $H \ll 1$, $\hat{\psi}_{xt}$ is a good approximation to ψ_{xt}, i.e.,

$$|\hat{\psi}_{xt}| \gg |H\psi_{Ix(0)t}|,$$

so that the contribution to ψ_{xt} from the interior variable may be neglected near the coast.

With the weak-slope approximation, on the other hand, (A11) and (A12) still hold, but from (A10) we obtain

$$\hat{\psi}_{xt} = -\tau\delta_B^{-1}(1 - x), \quad \text{(A14)}$$

which gives

$$\psi_{xt} = -\tau\delta_B^{-1}(1 - x) - H\tau = -\tau. \quad \text{(A15)}$$

In this case,

$$|\hat{\psi}_{xt}| \ll |H\psi_{Ix(0)t}|$$

everywhere on the shelf so that the contribution of the interior variable to ψ_{xt} is not negligible. We can see, therefore, that for the weak-slope geometry in the two-dimensional limit, approximate equations for the shelf in which the contribution of the interior variables is neglected would lead to erroneous results and the possibly puzzling inability to recover a familiar limit.

To make the weak-slope problem in Section 4 more similar to that with a full slope, we choose a wind stress of the form (2.15), i.e.,

$$\tau^x = 0, \quad \tau^y \neq 0, \quad \tau_x{}^y = 0, \quad \tau_y{}^y \neq 0, \quad \text{(A16)}$$

which minimizes the importance of the interior variables.

Estimates of the resulting magnitudes of $\psi_{Ix(0)}$ and $h_{I(0)}$ may be obtained from (3.14b) and (3.17) in Section 3 and are

$$\psi_{Ix(0)} = O(\tau_0\hat{\alpha}), \quad h_I = O(a\delta_R{}^2 l_0\psi_{Ix(0)}). \quad \text{(A17a, b)}$$

It follows that

$$F_1 = \tau_{(0)}^{\gamma}[1 + O(l_0) + O(\alpha)], \quad \text{(A18a)}$$

$$F_2 = \tau_{(0)}^{\gamma}[1 + O(a\alpha)]. \quad \text{(A18b)}$$

Making assumptions (2.12), (2.13) and (2.14), utilizing $F_1 = F_2 = \tau_{(0)}^{\gamma} = \tau$ in (A9) and (A10), and dropping the carets on $\hat{\psi}$ and $\hat{h}$, we obtain (4.1) and (4.2) in Section 4.

APPENDIX B

Two-Dimensional Flow

For wind-stress-forced motion which is purely two-dimensional ($\partial/\partial y \equiv 0$) on a shelf with a vertical wall at the coast such that $H_{(0)} > H_1$, an approximate solution may be easily obtained for otherwise arbitrary $H(x)$ if

$$a_{(0)} = H_1/H_{2(0)} \ll 1 \quad \text{and} \quad H(x) \geqslant H_{(0)}.$$

In this case, (A10) with $\tau^y = \tau(t)$ may be written as

$$(\psi_x/H)_{xt} + \alpha[(\psi_x - h_x)/H^2]_x = -(\tau/H)_x, \quad \text{(B1)}$$

which may be integrated with respect to x to give

$$\psi_{xt} + \alpha_H \psi_x = -\tau + \alpha_H h_x, \quad \text{(B2)}$$

where $\alpha_H = \alpha/H$.

For $a_{(0)} \ll 1$, ψ and h are expanded in powers of $a_{(0)}$:

$$\left.\begin{aligned} \psi &= \psi_0 + a_{(0)}\psi_1 + \cdots \\ h &= h_0 + a_{(0)}h_1 + \cdots \end{aligned}\right\}, \quad \text{(B3)}$$

which when substituted in (A1b) and (A2b) give

$$(h_{0xx} - \hat{\delta}_R^{-2} h_0)_t = 0, \quad \text{(B4)}$$

$$h_{0xt} = -\tau \quad \text{at} \quad x = 0, \quad \text{(B5)}$$

where

$$\hat{\delta}_R^{\,2} = SH_1 = \delta_{R(0)}^2(1 + a_{(0)}).$$

For

$$\tau = \tau_0 \exp(i\sigma t), \quad \text{(B6)}$$

$$(\psi, h) = (\phi, g)\exp(i\sigma t), \quad \text{(B7)}$$

we obtain, with $\hat{r} = \hat{\delta}_R^{-1}$,

$$\phi_x = -\tau_0[i\sigma + \alpha_H]^{-1}[1 + (\alpha_H/i\sigma)e^{-\hat{r}x}], \quad \text{(B8a)}$$

$$g_x = -(\tau_0/i\sigma)e^{-\hat{r}x}. \quad \text{(B8b)}$$

Based on the exact solution (3.15) of the two-dimensional flat-bottom example in Section 3, we anticipate that the $O(a\alpha)$ frictional terms in (A2b) will not alter the balance in (B5) as $\sigma \to 0$ and thus not affect the $(i\sigma)^{-1}$ dependence of g_x in (B8b).

The velocity components, to lowest order in a, are

$$\tilde{u}_1 = (H_2/H)\tau_0(1 - e^{-\hat{r}x}), \quad \text{(B9a)}$$

$$\tilde{v}_1 = (H_2/H)(\tau_0/i\sigma)e^{-\hat{r}x}, \quad \text{(B9b)}$$

$$\tilde{u}_2 = -a\tilde{u}_1, \quad \text{(B9c)}$$

$$\tilde{v}_2 = (H_1/H)[\tau_0/(i\sigma + \alpha_H)](1 - e^{-\hat{r}x}), \quad \text{(B9d)}$$

In the flat-bottom limit $H = 1$, (B9) reduces to (3.16). Note that, as in (3.16), for a fixed value of σ an increase in α decreases $|\tilde{v}_2|$, but leaves $|\tilde{v}_1|$ unaffected.

APPENDIX C

Arrested Topographic Wave

The term "arrested topographic wave" has been coined by Csanady (1978) to describe the steady or quasi-steady solution for linear, wind-stress-forced motion of a barotropic fluid over sloping continental shelf and slope topography with bottom friction and with the assumption $l_0 \ll 1$ (2.11). Similar physics arose in earlier studies of Birchfield (1972, 1973) and Pedlosky (1974b). For reference, it is useful to examine briefly the corresponding "arrested topographic wave" solution in the present weak-slope geometry with the Heaviside-function wind stress of Section 4b:

$$\tau^y = \tau = \tau_0 \hat{H}(-y). \quad \text{(C1)}$$

The governing equation, obtained from (4.1a), is

$$\delta_B^{-1}(\psi_y - \tau) + \alpha\psi_{xx} = 0, \quad \text{(C2)}$$

with boundary conditions

$$\psi_y(x = 0) = 0, \quad \psi_x(x = 1) = 0. \quad \text{(C3a, b)}$$

We recognize (C2) as a forced diffusion equation with diffusion coefficient $\kappa = \alpha\delta_B$. The time-like direction is represented by $-y$. With boundary conditions (C3a, b), the solution may be conveniently found by expanding ψ and τ in terms of cross-shelf modes as in (4.20), (4.22) and (4.23). For τ given by (C1) and $\psi = \Sigma\, Y_n(y)\phi_n(y)$, we find that Y_n is given by (4.27b).

It is more illuminating, however, to consider the solution in the region $0 < -y \ll (\alpha\delta_B)^{-1}$, where the boundary condition (C3b) at $x = 1$ does not appreciably influence ψ. An approximate solution in that case may be obtained by changing condition (C3b) to

$$\psi_y - \tau \to 0 \quad \text{as} \quad x \to \infty. \quad \text{(C4)}$$

We define

$$\hat{\psi}_y = \psi_y - \tau \triangleq \hat{G}(y, x), \quad \text{(C5)}$$

so that $\hat{\psi}$ represents a streamfunction for the flow beneath the surface Ekman layer. It follows that

$$-\hat{G}_y = \kappa\hat{G}_{xx}, \quad \text{(C6a)}$$

$$\hat{G}(x = 0) = -\tau_0\hat{H}(-y), \quad \hat{G} \to 0 \text{ as } x \to \infty, \quad \text{(C6b, c)}$$

which is the same form as the classical Rayleigh problem, and thus that

$$\hat{G} = \hat{\psi}_y = -\tau_0 \operatorname{erfc}[x/(-4\kappa y)^{1/2}]. \quad \text{(C6d)}$$

Consequently, the flow beneath the surface Ekman layer is confined to a boundary layer in x originating

at $y = 0$ and growing in width in the negative y-direction as $\delta_x \approx (-\kappa y)^{1/2}$.

We note that the solution in the present weak-slope model with a vertical coast differs from that in the wedge-slope region, $H = \delta_B{}^{-1}x$, considered by Csanady (1978). The diffusion equation (C6a) is obtained in both cases, but the identification of variables and the boundary condition at the coast are different. In the wedge geometry, (C6) applies with $G = v$. The resulting flow field is different in detail, but both geometries have the motion beneath the surface Ekman layer confined to the parabolic region $\delta_x = (-\kappa y)^{1/2}$.

REFERENCES

Allen, J. S., 1973: Upwelling and coastal jets in a continuously stratified ocean. *J. Phys. Oceanogr.*, **3**, 245–257.

——, 1975: Coastal trapped waves in a stratified ocean. *J. Phys. Oceanogr.*, **5**, 300–325.

——, 1976: On forced, long continental shelf waves on an *f*-plane. *J. Phys. Oceanogr.*, **6**, 426–431.

——, 1980: Models of wind driven currents on the continental shelf. *Annual Reviews, in Fluid Mechanics*, Vol. 12, Annual Reviews 389–433.

——, and R. D. Romea, 1980: On the coastal trapped waves at low latitudes in a stratified ocean. *J. Fluid Mech.*, **98**, 555–585.

Anderson, D. L. T., and A. E. Gill, 1975: Spin up of a stratified ocean, with applications to upwelling. *Deep-Sea Res.*, **22**, 583–596.

Birchfield, G. E., 1972: Theoretical aspects of wind-driven currents in a sea or lake of variable depth with no horizontal mixing. *J. Phys. Oceanogr.*, **2**, 355–362.

——, 1973: An Ekman model of coastal currents in a lake or shallow sea. *J. Phys. Oceanogr.*, **3**, 419–428.

Brink, K. H., 1982: The effect of bottom friction on low-frequency coastal trapped waves. *J. Phys. Oceanogr.*, **10**, 765–778.

Csanady, G. T., 1978: The arrested topographic wave. *J. Phys. Oceanogr.*, **8**, 47–62.

Enfield, D. B., and J. S. Allen, 1980: On the structure and dynamics of monthly mean sea level anomalies along the Pacific coast of North and South America. *J. Phys. Oceanogr.*, **10**, 557–578.

Gill, A. E., and E. H. Schumann, 1974: The generation of long shelf waves by the wind. *J. Phys. Oceanogr.*, **4**, 83–90.

Grant, W. D., and O. S. Madsen, 1979: Combined wave and current interaction with a rough bottom. *J. Geophys. Res.*, **84**, 1797–1808.

Huyer, A., R. L. Smith and E. J. C. Sobey, 1978: Seasonal differences in low-frequency current fluctuations over the Oregon continental shelf. *J. Geophys. Res.*, **83**, 5077–5089.

Martinsen, E. A., and J. E. Weber, 1981: Frictional influence on internal Kelvin waves. *Tellus*, **33**, 402–410.

Mofjeld, H. O., 1980: Effects of vertical viscosity on Kelvin waves. *J. Phys. Oceanogr.*, **10**, 1039–1050.

Pedlosky, J., 1974a: Longshore currents and the onset of upwelling over bottom slope. *J. Phys. Oceanogr.*, **4**, 310–320.

——, 1974b: Longshore currents, upwelling, and bottom topography. *J. Phys. Oceanogr.*, **4**, 214–226.

Romea, R. D., and J. S. Allen, 1982: On forced coastal trapped waves at low latitudes in a stratified ocean. *J. Mar. Res.*, **40**, 369–401.